Journal of Undergraduate Chemistry Research, **2025**, 24 (3), 66

ENHANCED FLUORESCENCE OF NAPHTHALENE ON Al_2O_3 BY 1,ω–DICHLOROALKANES

Brandon X. Moses*, Caleb D.Tobey,* Alan O. Lopez* and A.M. Nishimura†

Department of Chemistry, Westmont College, Santa Barbara, CA 93108

Abstract

Physical vapor deposition of aromatic hydrocarbons on Al_2O_3 form adsorbates that are initially amorphous but undergo disorder-to-order transition when the temperature of the substrate is ramped during the temperature programmed desorption (TPD) experiment. In bilayers where the overlayer is naphthalene, a fluorophore, the underlayer can be used to disrupt the morphology of the overlayer and this disruption can be observed by monitoring its fluorescence during the TPD. Homologous series of 1,ω-dichlorohexane was found to enhance the naphthalene fluorescence from both excimer and traps.

†Corresponding author: nishimu@westmont.edu *Undergraduate researchers and co-authors

Keywords: adsorption, naphthalene, excimer, vapor deposition, desorption, temperature programmed desorption, TPD

Submitted: July 1, 2025 Accepted: July 6, 2025 Revision submitted: July 7, 2025 Pubished: July 9, 2025

Introduction

Due to dispersion forces, vapor deposited 1-chloroalkanes on Al_2O_3 aggregated to form adsorption sites if the length of the alkyl moiety was sufficient to accommodate the fluorophore laid on top.[1-6] This finding motivated an ancillary question: by careful choice of the underlayer, can the fluorophore be made to form a specific *type* of fluorescence emitter, namely trap or excimer, as the underlayer percolated through the fluorophore on its way to desorption?[1] Any effect on excimer or trap fluorescence should be manifested by changes in these sources of emission. 1,6-Dichlorohexane was an example of an underlayer that promoted the formation of traps after the disorder-to-order transition of biphenyl.[1,2] Hence any effect on excimer or trap fluorescence should be manifested by changes in these sources of emission.

In a recent study, biphenyl was used to characterize the change in surface morphology that was caused by a homolgous series of 1,ω-dichloroalkanes.[7] The change caused by the dichloroalkanes was significantly larger than the corresponding unsubstituted alkanes and tentatively attributed to the π-Cl interaction that can occur between the dichloralkane and biphenyl.[8,9] The π-Cl interaction has been attributed to the electrostatic interaction between the positive σ-hole on the chlorine and the negative electronic density of the aromatic rings.[8,9] Another observation was that as the 1,ω-dichloroalkane moved through the biphenyl adlayer, the Cl-π interaction caused the biphenyl that was in the ordered state to fracture in its wake, thereby increasing the density of defect sites from which radiative relaxation can occur.[7] Thus this interaction caused the fluorophoric intensity to increase.[7]

During the TPD experiment, vapor deposited hydrocarbons on a surface underwent disorder-to-order transitions. For example, vapor deposited biphenyl on Al_2O_3 is initially in the twisted conformer, which is consistent with its conformer in the vapor phase.[10-14] When it undergoes the disorder-to-order transition about midway through the TPD, it becomes nearly planar.[10-14] Vapor deposited naphthalene on Al_2O_3, on the other hand, formed energetically stable excimer that did not undergo the usual disorder-to-order transition until just a few degrees before desorption.[14]

The aim of this study was to determine if the π-Cl interaction due to 1,ω-dichloroalkanes in the biphenyl study, could effectively overcome the stability of the naphthalene excimer and cause the excimer-to-order transition as the underlayer percolated through the naphthalene overlayer as it underwent desorption.

Experimental

Naphthalene, 1,ω-dichloroalkanes and 1,4-dibromobutane of the highest purity (> 99%) were purchased from commercial sources (Sigma-Aldrich, St. Louis, MO; TCI, Portland, OR). They were placed in a sample holder attached to one end of a precision leak valve for vapor deposition. The ultra-high vacuum chamber had a background hydrogen base pressure of 1×10^{-9} Torr. A single crystal of Al_2O_3 (0001) (Crystal Systems, Inc., Salem, MA) was suspended on the lower end of a liquid nitrogen cryostat via copper post on either side of the Al_2O_3 with a sapphire spacer for both electrical and some degree of thermal isolation from the cryostat. Resistive heating of the Al_2O_3 was done by sending current through a thin tantalum foil that was in thermal contact with the substrate. A type-K (chromel/alumel) thermocouple (Omega, Norwalk, CT) that was also in thermal contact with the Al_2O_3 monitored the temperature. Process control during the TPD experiment was accomplished by a program written in LabVIEW (National Instruments, Austin, TX) that incorporated a PID (proportional-integral-derivative) feedback algorithm that linearly incremented the temperature of the Al_2O_3 crystal at 1.98 ± 0.01 K s^{-1} (roughly 2 K s^{-1}).

Optical pumping of the fluorophore was accomplished with a high pressure Hg lamp whose output was focussed through a 0.25 m monochrometer and λ_0 was set at 250 nm. Fluorescence emission from the adlayer on the Al_2O_3 was captured via a quartz lens and light pipe assembly was attached to the vacuum feedthrough that terminated at the spectromer. During the TPD, the LabVIEW program took the fluorescence spectra every 300 ms in real time from an Ocean Optics USB4000 spectrometer (Ocean Optics, Dunedin, FL) that was sensitive in the ultra-violet. Manipulation of the array of spectra as a function of temperature by a MATLAB (Mathworks, Natick, MA) template yielded the WRTPD (wavelength-resolved TPD) that are shown in the figures. To ensure a clean surface, the Al_2O_3 was heated to 300 K after each run. Temperature ramps to higher temperatures did not indicate any other adsorbates.[10-14]

The activation energy for desorption, E_a, was calculated by Redhead analysis in which a first-order desorption kinetics as de-

scribed by King was assumed and is based on the mass spectral peak desorption temperature, T_p.[15-17] The uncertainties in the desorption temperatures lead to a propagated error in the activation energies of ± 2%.

The LabVIEW program received data from a residual gas analyzer so that both the deposition and the desorption of naphthalene could be monitored. The surface coverages, Θ, in monolayers (ML) were calculated by calibrating the integrated mass spectral peaks in an optical interference experiment. The interference experiment yielded accurate rate of deposition with coverage error of ± 30%, and is described in detail elsewhere .[10-14]

Transmittance of the excitation light was detected with a photomultiplier whose output was sent to a computer interfaced high resolution analog-to-digital converter that the same LabVIEW program controlled. A UV shortpass optical filter had been placed in front of the photomultiplier (PMT) detector so that only the 250 nm excitation light was being monitored. The voltages from the photomultiplier at 0% and 100% transmittances were determined by blocking the excitation light and using the same optical configuration with a clean surface, respectively. In this way, the transmittance correlated linearly with the voltages from the photomultiplier. Sources of error are the fluctuation in the excitation light and PMT that gave low frequency and high frequency noise, respectively, and resulted in ± 3% error in the % transmittance.

For surface coverages in the multilayer regime, multidimensional nucleation and crystal growth are expected at the disorder-to-order transition. In order to model the disorder-to-order transition as a nucleation-crystallization process, the Avrami model was used.[18] The Avrami equation is given by:

$$I(t) = e^{-kt^n}$$

where $I(t)$ is the time dependent fluorescence intensity at the disorder-to-order transition that is converted to fraction of the disordered state at the transition, k is related to the rate with which crystallization occurs and is in part, a function of the density of nucleation sites, **t** is time in s and n is the dimensionless Avrami exponent that yields the dimensionality of the nucleation-crystallization process.[18] The unit for k is the inverse of time raised to the n^{th} power.[18] This expression was made to fit the wavelength-resolved TPD data at the disorder-to-order transition using algorithms provided by SciPy (an open-source Python library) and automated with Python (an open-source programming language, Python Software Foundation) in which the parameters were controlled by user interface.

A 10 Hz pulsed quadrupled Nd:YAG laser with output at 266 nm was the excitation source for the laser-induced fluorescence, LIF, measurements. The fluorescence was focused with short focal length lens onto a 0.25 m monochromator equipped with a photomultiplier and λ_0 was set at 398 nm, the peak of the naphthalene excimer fluorescence. The signal from the photomultiplier was amplified and sent to a very fast digitizing oscilloscope, averaged over 4 LIF decay scans and the waveform was exported to the controlling computer that was running the LabVIEW program. The LIF was assumed to decay by first-order kinetics. A least square curve-fitting program was used to determine the slope, i.e. the rate constant, and intercept of this line during the TPD experiment. The intercepts are the initial intensities of the LIF decay. About 2 replicates of TPD runs yielded LIF decay rate constants with a precision of about ± 10%.

Results and Discussion

Physical vapor deposition of naphthalene resulted in an physisorbed, amorphous arrangement of adsorbate molecules in the adlayer as evidenced by spectral signature of an excimer fluorescence.[19] During the TPD, the adsorbate transitioned from the amorphous morphology to a more ordered state.[10-14] In a bilayer, if the underlayer has a lower desorption temperature than the overlayer, the underlayer molecules will percolate through the overlayer before desorbing during the TPD procedure.[1,10-14] Desorption temepratures and activation energies for desorption are summarized in Table 1.[15-17] The interaction with the underlayer molecules during percolation typically will have an effect on the morphology of the fluorophoric adlayer. By judicious choice of the underlayer, the morphology of the overlayer could be manipulated in such a way that ordering in the orderlayer can be forced to occur. This might occur by causing nucleation sites or if the overlayer is ordered when the underlayer comes through, it can be fractured, thereby increasing the density of defect sites from which radiative relaxation can occur. The result is enhanced monomeric fluorescence.[20] A third way with which the underlayer can affect the overlayer is by increasing the distance between the fluorophoric molecules. Aggregation quenching is reduced and the fluorescence quantum yield would be enhanced.[19]

Multilayer naphthalene

Shown in Figure 1 is the wavelength-resolved TPD of naphthalene. The adlayer that forms when naphthalene is vapor deposited on Al_2O_3 is amorphous. Optical pumping of the singlet elec-

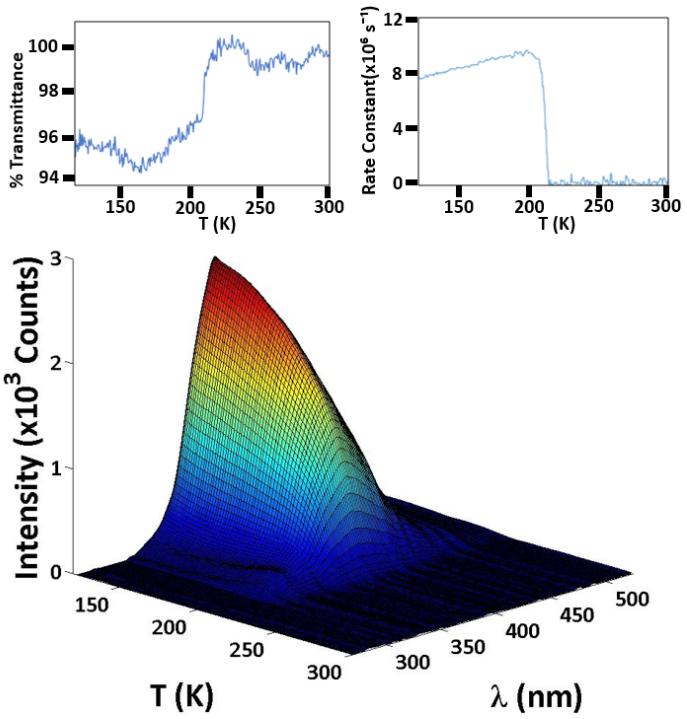

Figure 1. Wavelength-resolved TPD of naphthalene neat with coverage of 97 ML. The excimer has a λ_{max} = 398 nm. The excimer-to-order transition occurs at 200 K during the TPD, but the trap emission from the ordered state is barely visible. Left inset: % transmittance vs. T during the TPD. Right inset: LIF rate constant vs T during the TPD.

tronic state gave rise to excimer fluorescence with λ_{max} = 398 nm that has been so categorized because of the observed broad and featureless spectrum.[19] As the temperature of the Al_2O_3 substrate was increased in a TPD experiment, naphthalene underwent a disorder-to-order transition at about 200 K, at which temperature the spectrum changed to that observed for the monomer with two peaks at 325 and 334 nm. The doublet was due to the strong vibrational progression that has been attributed to a C-H bending vibration.[19]

The left inset in Figure 1 shows that the measured transmittance does not fall below about 4% with a signal-to-noise ratio of of 1:1. The fluorescence intensity is relatively high even with very low absorption of the excitation light. This would be indicative of very high quantum yield for the naphthalene excimer.

The right inset in Figure 1 shows the fluorescence rate constant to increase monotonically from about $7.8x10^6$ to $9.4x10^6$ s^{-1}. The increase is attributed to thermally induced quenching, as can be seen from decreasing intensity of the excimer fluorescence. The lifetimes, the inverse of the rate constants, are consistent with those previously reported.[19]

Dichloromethane/naphthalene

Shown in Figure 2 is the wavelength-resolved TPD of naphthalene with an underlayer of dichloromethane. Upon deposition and prior to the temperature ramp, the intensity of the excimer was noticeably higher due to the presence of the underlayer (Cf. Figure 1). In effect, the dichloromethane's surface upon which naphthalene was deposited separated the amorphous molecules so that the intermolecular interactions were less, which in turn lowered aggregation-caused quenching.

The left inset in Figure 2 shows that the transmittance was considerably lower than when the underlayer was absent (Cf. left inset of Figure 1). At the start of the TPD, the transmittance was about 80%. When the dichloromethane desorbed, the transmittance dipped due to scattering of the excitation light, with the concomitant increase in the excimer intensity. Some excimer-to-trap ordering was evidenced at that temperature as indicated by the blue-shifted fluorescence. Notice that the scattering did not affect the fluorescence intensity; this has been observed in all of the bilayer systems (*Vide infra*). From the right inset, the fluorescence rate constant was observed to be 30% lower due to a decrease in aggregation-caused quenching as noted above. Due to thermally induced quenching, the fluorescence rate constant shown in the right inset began at about $6x10^6$ s^{-1} and increased monotonically to about $8.5x10^6$ s^{-1}. When the dichloromethane desorbed, the rate constant dipped by about 17% due to the separation on the excimer molecules. The postulate is that separation of fluorophore lowers quenching due to molecular aggregation.

1,2-Dichloroethane/naphthalene

Shown in Figure 3 is the wavelength-resolved TPD of a bilayer of 1,2-dichloroethane and naphthalene. The underlayer was annealed at 130 K for 30 s. Annealing the underlayer is known to increase the intensity of the naphthalene fluorescence. So that procedure was followed in this study, with the exception of dichloromethane and 1,3-dichloropropane underlayers. Notice again, that the intensity of the excimer fluorescence was higher for the same reason as in the dichloromethane/naphthalene system, i.e. separation effect. From the left inset, the transmittance which was 90% initially, was considerably lower than that the 96% for multilayer (Cf. Figure 1, left inset).

1,3-Dichloropropane/naphthalene

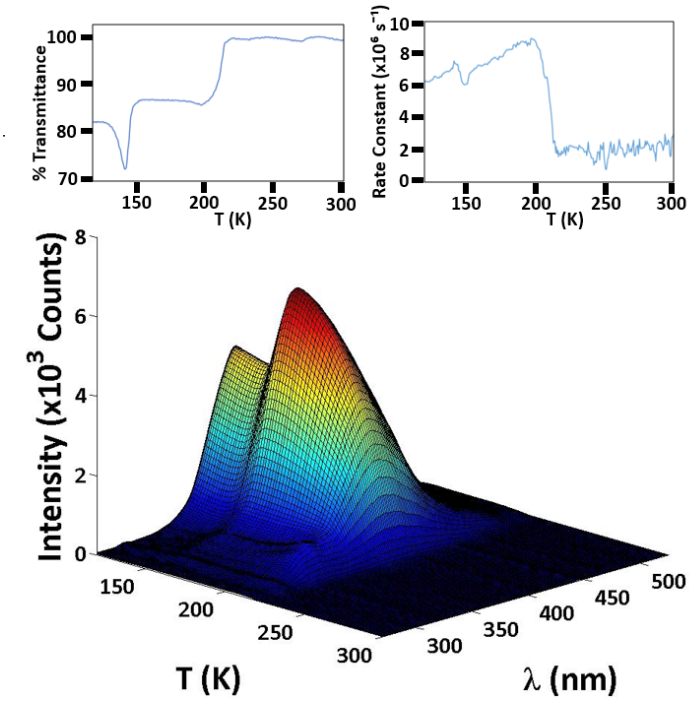

Figure 2. Wavelength-resolved TPD of naphthalene with $\Theta_{naphthalene}$ = 87 ML that had been deposited at 117 K with an underlayer of dichloromethane with $\Theta_{dichloromethane}$ = 102 ML that was not annealed. Left inset: % transmittance vs. T during the TPD. Right inset: LIF rate constant vs T during the TPD.

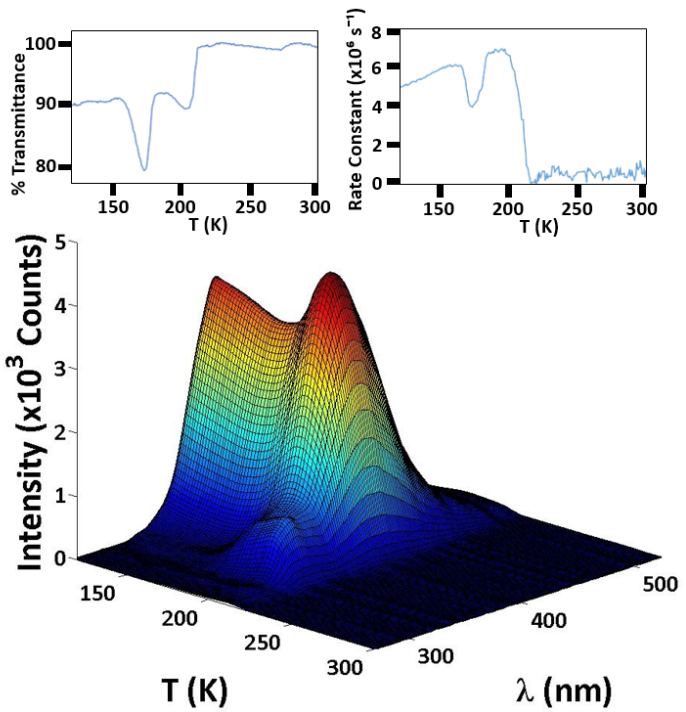

Figure 3. Wavelength-resolved TPD of naphthalene with $\Theta_{naphthalene}$ = 89 ML with an underlayer of 1,2-dichloroethane with $\Theta_{1,2\text{-dichloroethane}}$ = 253 ML that had been annealed at 130 K for 30 s. Left inset: % transmittance vs. T during the TPD. Right inset: LIF rate constant vs T during the TPD.

Shown in Figure 4 is the wavelength-resolved TPD of a bilayer of 1,3-dichloropropane and naphthalene. What is interesting here is that this particular underlayer has very little effect on the excimer fluorescence of naphthalene. This is tentatively attributed to the even-odd effect of alkanes[20,21] that was reported for these 1,ω-dichloroalkanes with biphenyl.[7] The transmittance and rate constants as seen in the left and right insets, respectively were very similar to the 1,2-dichloroethane.

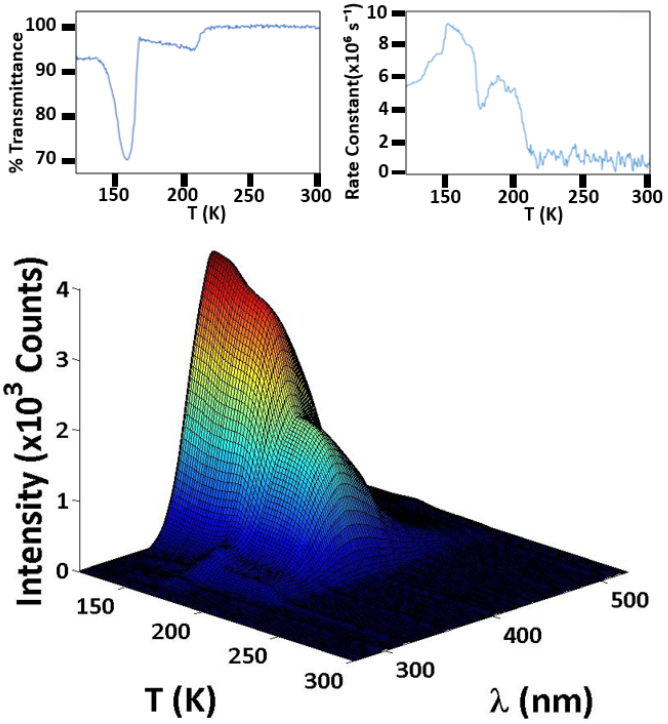

Figure 4. Wavelength-resolved TPD of naphthalene with $\Theta_{naphthalenel}$ = 92 ML with an underlayer of 1,3-dichloropropane with $\Theta_{1,3\text{-dichloropropane}}$ = 220 ML that was not annealed. Left inset: % transmittance vs. T during the TPD. Right inset: LIF rate constant vs T during the TPD.

1,4-Dichlorobutane/naphthalene

Shown in Figure 5 is the wavelength-resolved TPD of a bilayer of 1,4-dichlorobutane and naphthalene. The excimer intensity was enhanced as the 1,4-dichlorobutane percolated and passed through the naphthalene. As it did so, the rate constant decreased momentarily during the TPD experiment. This has been postulated to be due to the separation of the fluorophoric molecules due to the passage of the 1,4-dichlorobutane. Simultaneously the transmittance decreased as has been observed in the previous bilayers.

1,5-Dichloropentane/naphthalene

Figure 6 is the wavelength-resolved TPD for the bilayer consisting of 1,5-dichloropentane and naphthalene. The effect of the underlayer qualitatively appears muted, compared to 1,4-dichlorobutane, and has been tentatively attributed to the previously mentioned even-odd effect in alkanes.[20-21]

1,6-Dichlorohexane/naphthalene

Figure 7 shows the wavelength-resolved TPD of naphthalene with an underlayer of 1,6-dichlorohexane . What was immediately apparent was that the trap emission was significantly enhanced by the desorption of 1,6-dichlorohexane at 212 K during the TPD. For naphthalene, 1,6-dichlorohexane created sufficient nucleation sites so that the excimer molecules were induced to crystallize out.

1,8-Dichlorooctane/naphthalene

Figure 8 shows the wavelength-resolved TPD of the bilayer of 1,8-dichlorooctane and naphthalene. Here, the underlayer de-

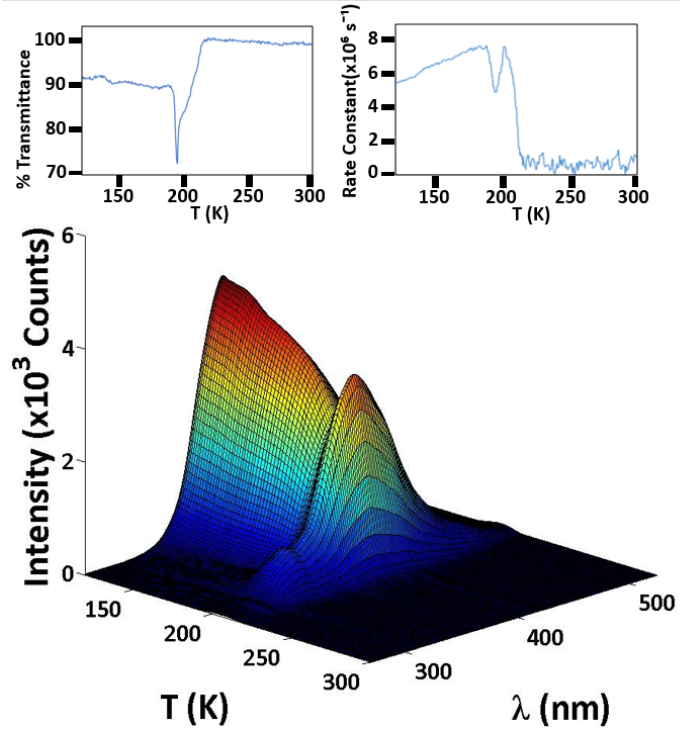

Figure 5. Wavelength-resolved TPD of naphthalene with $\Theta_{naphthalenel}$ = 104 ML with an underlayer of 1,4-dichlorobutane with $\Theta_{1,4\text{-dichlorobutane}}$ = 220 ML that had been annealed at 130 K for 30 s. Left inset: % transmittance vs. T during the TPD. Right inset: LIF rate constant vs T during the TPD.

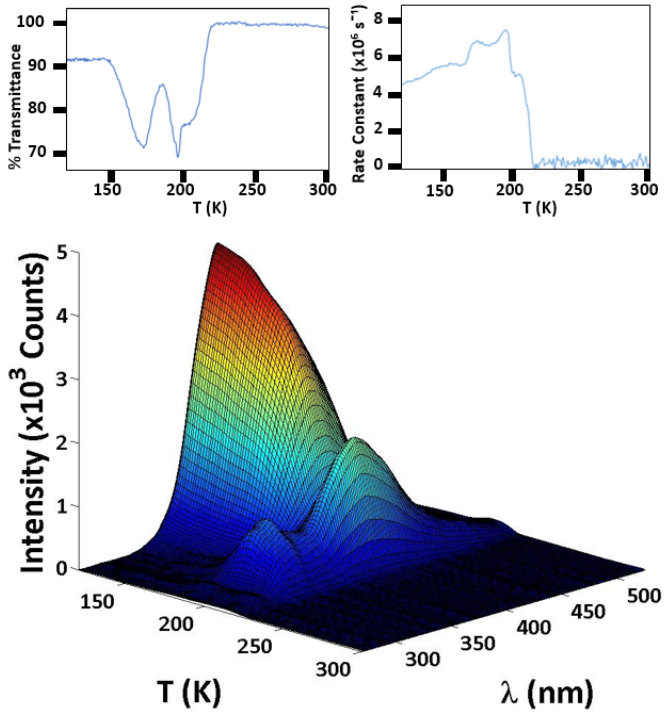

Figure 6. Wavelength-resolved TPD of naphthalene with $\Theta_{naphthalenel}$ = 102 ML that with an underlayer of 1,5-dichloropentane with $\Theta_{1,5\text{-dichloropentane}}$ = 208 ML that had been annealed at 130 K for 30 s. Left inset: % transmittance vs. T during the TPD. Right inset: LIF rate constant vs. T during the TPD

sorbed *after* the naphthalene. Therefore its effect was minimal, as can be seen from the figure.

Effect of underlayer on the kinetics of the excimer-to-ordered transition due to the nucleation-crystallization in naphthalene

The *average* values of *k* and *n* are summarized in Figure 9 for the 1,ω-dihaloalkanes. The dimensionality of the nucleation appears relatively constant ($2 < n < 3.5$) while the *k* value vary. Both the *n*- and *k*-values and their errors are shown in Table 1. Trend appears lacking, however.

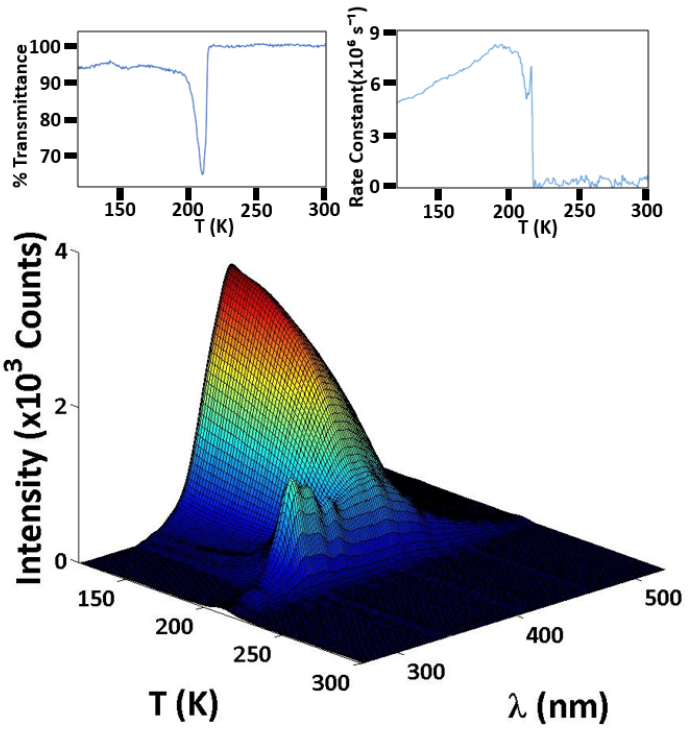

Figure 7. Wavelength-resolved TPD of naphthalene with $\Theta_{naphthalene}$ = 112 ML that with an underlayer of 1,6-dichlorohexane with $\Theta_{1,6\text{-dichlorohexane}}$ = 93 ML that was annealed at 160 K for 30 s. Left inset: % transmittance vs. T during the TPD. Right inset: LIF rate constant vs. T during the TPD.

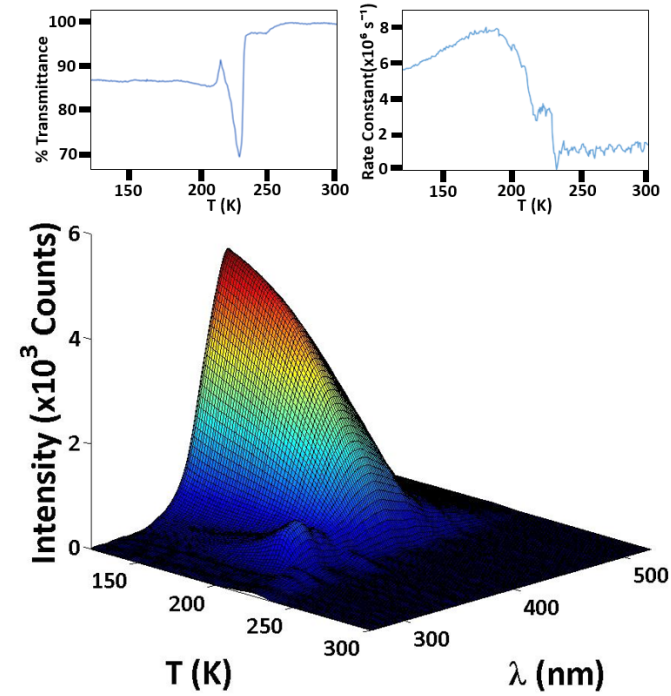

Figure 8. Wavelength-resolved TPD of naphthalene with $\Theta_{naphthalene}$ = 88 ML that with an underlayer of 1,8-dichlorohexane with $\Theta_{1,8\text{-dichlorohexane}}$ = 241 ML that had been annealed at 200 K for 30 s. Left inset: % transmittance vs. T during the TPD. Right inset: LIF rate constant vs T during the TPD

Summary

The general strength of Cl-π interaction has been reported to be about 8.4 kJ mol^{-1}.[8,9] The thermal energy available for the excimer when it undergoes the excimer-to-order transition is about 2 kJ mol^{-1}. It would appear that the transition barrier decreased with temperature such that for 1,6-dichlorohexane which has the highest T_p in this series of 1,ω-dichloroalkanes, the Cl-π interaction was sufficient to not only induce the transition, but increase the density of defect sites. This is manifest by the increase in the trap emission (Cf. Figure 7).

Based on the observed enhanced naphthalene fluorescence upon the passage of the 1,ω-dichloroalkanes and the difficulty with which the excimer-to-order transition was induced, if at all, the naphthalene excimer can be concluded to be energetically stable. It is possible that the mutual repulsion of the chlorines on the terminal ends of the alkyl moiety does not allow an efficient Cl-π interaction. When comparing naphthalene with biphenyl, it is possible that the differences can be attributed to the fact that the two π-rings

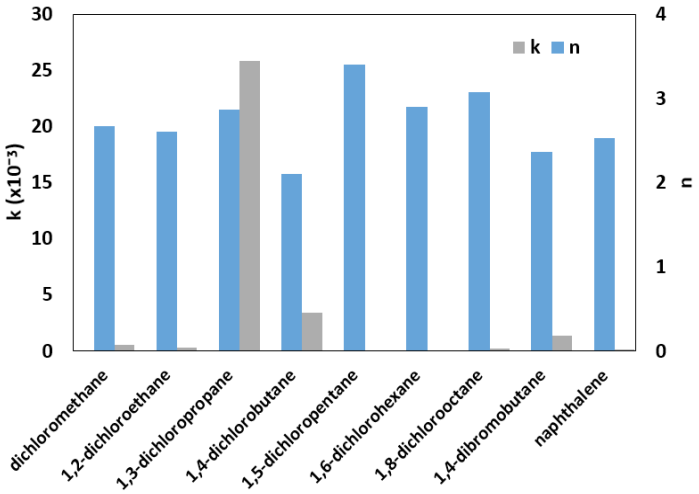

Figure 9: *Average* Avrami *k* and *n* values for the crystallization kinetics of naphthalene with the 1,ω-dihaloalkanes that were studied. The *n* values remained relatively constant between $2 < n < 3.5$, whereas the *k* values are widely varied. Avrami n-values and errors in *n* along with *k*-values and errors in *k* are shown in Table 1.

Table 1: Summary of peak desorption temperatures, T_p (K) and energy of activation of desorption, E_a (kJ/mol) for the adsorbates in this study. Avrami *n*- and *k*- values are also shown.

Underlayer	T_p (K)	E_a (kJ/mol)	Avrami n	Avrami k
dichloromethane	144 ± 5	39 ± 1	3 ± 0.3	$6 \pm 10 \cdot 10^{-4}$
1,2-dichloroethane	173 ± 10	44 ± 2	3 ± 0.5	$3 \pm 4 \cdot 10^{-4}$
1,3-dichloropropane	165 ± 1	42.3 ± 0.2	3 ± 1	$3 \pm 4 \cdot 10^{-2}$
1,4-dichlorobutane	188 ± 9	49 ± 2	2 ± 0.4	$3 \pm 7 \cdot 10^{-3}$
1,4-dibromobutane	207 ± 11	54 ± 3	2 ± 0.2	$13 \pm 7 \cdot 10^{-4}$
1,5-dichloropentane	191 ± 3	49 ± 1	3 ± 0.5	$7 \pm 20 \cdot 10^{-5}$
1,6-dichlorohexane	212 ± 2	55.0 ± 0.4	3 ± 0.4	$6 \pm 7 \cdot 10^{-5}$
1,8-dichlorooctane	231 ± 1	60.0 ± 0.3	3 ± 0.7	$2 \pm 3 \cdot 10^{-4}$
naphthalene	212.1 ± 0.1	54.8 ± 0.01	3 ± 0.1	$10 \pm 7 \cdot 10^{-5}$

are adjacent in naphthalene, where in biphenyl, the two π-rings are separated by a C-C bond. Also, the initial biphenyl conformation is twisted which will allow a small twist in the two terminal chlorines, which would be more energetically favorable conformation for the 1,ω-dichloroalkanes. This conformation would allow *both* chlorines on the 1,ω-dichloroalkane to interact with the biphenyl's π-bonded rings.

For naphthalene, some Cl-π interaction is possible with one of the chlorines on the terminal end. This would serve to stablize the excimer, and is evidenced by the higher excimer fluorescence intensity before the chloroalkane desorbs. 1,6-Dichlorohexane is an exception only because its desorption temperature is the same as naphthalene. (Cf Table 1). The simultaneous desorption facilitates the excimer-to-trap transitionl, fracture any ordered naphthalene and the emission from traps is increased.

Acknowledgment

The authors would like to thank the John Stauffer Charitable Trust for funding the student stipends for summer research. This work was supported by the donorsof ACS Petroleum Research Fund under Undergraduate Research #68385-UR5 .

References

1. J.M. Rosenfeld, R.M. Toepfer, A.O. Lopez, J.C. Nieman, I. Felix, J. Zerwas and A.M. Nishimura, *JUCR*, **2024.** 23, **2024**.
2. I.Z. Song, S.T. Watanabe and A.M. Nishimura, *JUCR*, **2023**, 22, 78-85.
3. M. Frederick, J. Fowkes, *J. Phys. Chem*., **1980**, 84, 510-512.
4. M. Anwar, F. Turci and T. Schilling, *J. Chem. Phys.* **2013**, 139, 214904.
5. T. Arnold, C.C. Dong, R.K. Thomas, M.A. Castro, A. Perdigon, S.M. Clarke and A. Inaba, *Phys. Chem. Chem. Phys*.,**2002**, 4, 3430-3435.
6. T. Arnold, R.K. Thomas, M.A. Castro, S.M. Clarke, L. Messe and A. Inaba, *Phys. Chem. Chem. Phys*., **2002**, 4, 345-351.
7. A.O. Lopez, B.X. Moses, C.D. Tobey, J. Arrieta, M. Ticas, J. Zerwas amd A.M. Nishimura, *JUCR*, 2025, 24, 59-65.
8. K.E. Riley and K.A. Tran, *Crystals*, **2017**,7, https://doi.org/10.3390/cryst7090273.
9. K. Shimizu and J.F. da Silva, *Molecules*, **2018**, 23 2959. https://doi.org/10.3390/molecules23112959
10. M.K. Condie, Z.E. Moreau and A.M. Nishimura *JUCR*, **2019**, 18, 15-18.
11. M.K. Condie, B.D. Fonda, Z.E. Moreau and A.M. Nishimura, *Thin Solid Films*, **2020**, 697, 137823-137828.
12. B.D. Fonda, Z.I. Shih, J.J. Wong, L.G. Foltz, K.A. Martin and A.M. Nishimura, *JUCR*, **2018**, 17, 32-35.
13. K.L. Nili, Z.E. Moreau and A.M. Nishimura, *JUCR*, **2020**, 19, 19-23.
14. M.K. Condie, C. Kim, Z.E. Moreau, B. Dionisio, K. Nili, J. Francis, C. Tran, S. Nakaoka and A.M. Nishimura, *JUCR*, **2020**, 19, 14-17.
15. P.A. Redhead. *Vacuum*, **1962**, 12, 203-211.
16. F.M. Lord and J.S. Kittelberger. *Surf. Sci.*, **1974**, 43, 173-182.
17. D.A. King. *Surf. Sci*., **1975**, 47, 384-402.
18. M. Avrami, J. Chem. Phys. 1939, 7, 1103-1112; 1940, 8, 212-224.
19. J.B. Birks. *Photophysics of Aromatic Molecules*, John Wiley & Sons Ltd., New York, NY (1970), pp. 301-370.
20. Y.N. Imai, Y. Inouye, I. Nakanishi and K. Kitaura, *Protein Sci.* **2008**, 17, 1129-1137.
21. F. Tao and S.L. Bernasek, *Chemical Reviews,* **2007**, 107, 5, 1408-1453. https://doi.org/10.1021/cr050258d.
22. A.O. Lopez, J.C. Nieman, J.M. Rosenfeld, R.M. Toepfer and A.M. Nishimura, *JUCR*, **2024**, 23, 16-23.
23. G. Cavallo, P. Metrangolo, R. Milani, T. Pilati, A. Prilmagi, G. Resnati and G. Terraneo, *Chem. Rev.*, **2016**, 111, 2478-2601; https://doi.org/10.1021/acs.chemrev.5b00484.
24. K.E. Riley and K.A. Tran, *Crystals*, **2017**, 7, 273; https://doi.org/10.3390/cryst7090273.
25. R. Wilcken, M.O. Zimmerman, A. Lange, A.C. Joerger and F.M. Boeckler, *J. Med. Chem*. **2012**, 56, 1363-1388.: https://doi.org/10.1021/jm3012968,

---

Supplemental

Is Cl-π interaction important during the TPD of 1,ω-dichloroalkane with naphthalene?

The strength of halogen-π interaction increases in the order: F < Cl < Br < I because of increasing polarizability and the size of the σ-hole.[23-25] In order to substantiate the hypothesis that the halogen-π interaction was involved in increasing the fluorescence intensity of naphthalene during the TPD, a system with 1,4-dibromobutane underlayer was investigated to determine if its effect on naphthalene was more substantial than with 1,4-dichlorobutane (Compare Figures 5 and 10). Desorption of 1,4-dibromobutane occurred within 5 K of naphthalene (Cf. Table 1), and the effect was difficult to observe. The thermally induced quenching appeared to

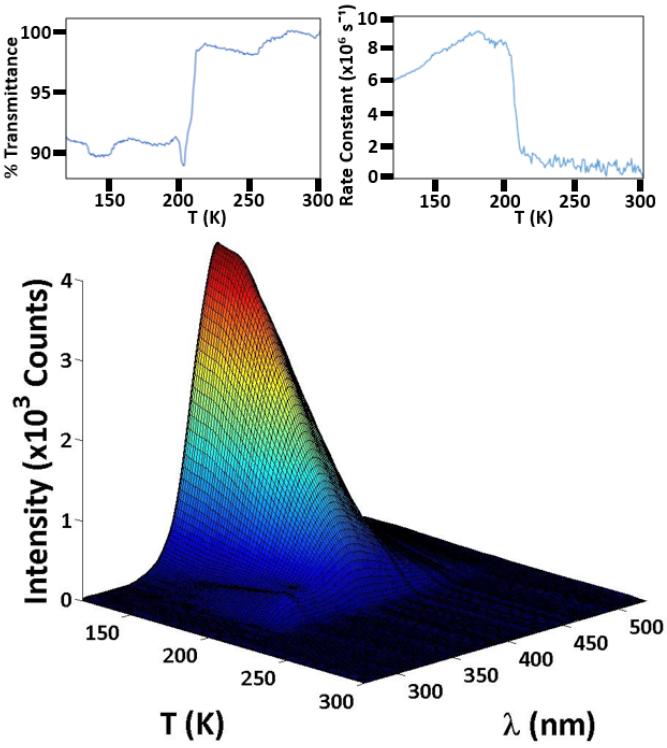

Figure 10. Wavelength resolved TPD of 1,4-dibromobutane/naphthalene bilayer with $\Theta_{1,4\text{-dibromobutane}}$ = 73 ML and $\Theta_{naphthalene}$ = 97 ML. Left and right insets are the % transmittance and the LIF rate constants as a function of temperature during the TPD, respectively.

be more pronounced than in the multilayer naphthalene. Initially, the thought was that since Cl-π interaction appeared to be effective for biphenyl, why not with naphthalene? However, it may be that the Cl-π interaction might not be as important for naphthalene as originally thought. See the explanationin the summary section above.

To further show that the Cl-π interaction was not as important as dispersion forces in the disruption of the naphthalene excimer intensity, hexane was used in the underlayer and the result is show in Figure 11. The observations were three-fold. The increase in the excimer intensity was due to decrease in aggregation-caused quenching. The excimer-to-order occurred to a greater extent, and the density of traps was increased within the ordered naphthalene. Note also that the transmittance was largely decreased and the LIF rates were lower than in the multilayer. All these occurred to even a greater extent, all in the absence of halogens in the terminal ends.

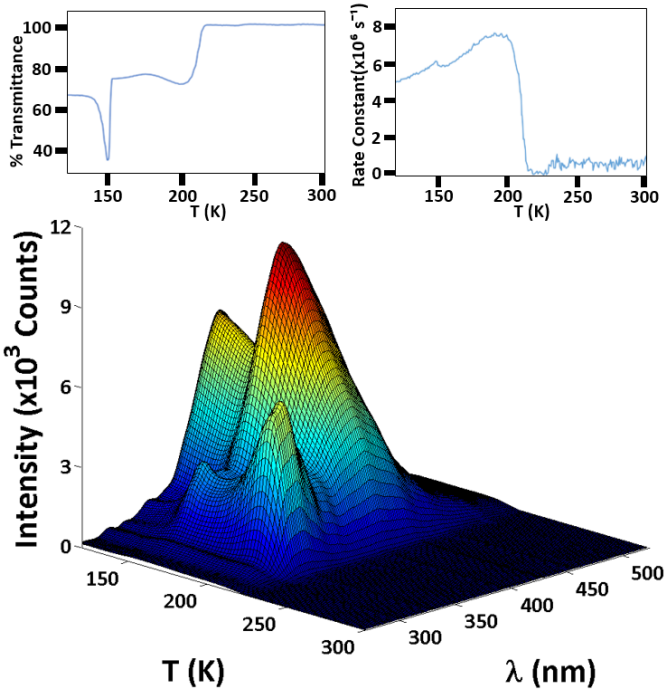

Figure 11. Wavelength resolved TPD of hexane/naphthalene bilayer with Θ_{hexane} = 209 ML and $\Theta_{naphthalene}$ = 100 ML. Left and right insets are the % transmittance and right the lifetimes as a function of temperature during the TPD, respectively.

Further insight into the effect of 1,ω-dichloroalkanes on the k and n values in the application of the Avrami model of crystallization kinetics on the excimer-to-order transition in naphthalene

In Figure 12, the Avrami *k*-values are plotted as a function of *n*-values for the 1,6-dichlorohexane/naphthalene bilayer. What was discovered was that when *k* was high, *n* was low and vice versa, and was an exponentially decaying relationship ($k = 1.85\pm0.05\bullet10^{-5}s^{-1}e^{-3.84\pm0.05n}$). This mathematical relationship was closely obeyed for all of the bilayers. In effect, the rate of crystal growth is exponentially related to the inverse of the dimensionality of the growth.

As mentioned above, the Avrami model applies well to the crystallization kinetics with 1,6-dichlorohexane underlayer to naphthalene. In particular, when the *k* is plotted as a function of *n*, the functional form of the plotted points is an exponentially decaying function of the form: $\mathbf{k = a\ e^{-bn}}$, for which the **a** = 1.61 ± 0.61 and **b** = 3.54 ± 0.20 for 1,2-dichloroethane, 1,4-dichlorobutane, 1,5-dichloropentane, 1,6-dichlorohexane and 1,8-dichlorooctane.

Dichloromethane with k = 4.13 and n = 3.62 and 1,3-dichloropropane with k = 0.584 and n=1.43 are slightly outside the range. Even so, when these are included, **a** = 1.82 ± 1.2 and **b** = 3.2 ± 0.82.

In some of the TPD, as in Figures 2 to 6, two rates of crystallization exist: before the underlayer desorbs, and after it desorbs, the former changes more slowly with temperature than the latter. These rates were analyzed separately, and are shown in Figure 13. Noteably the larger *k* with the smaller *n* occurred *before* desorption and the smaller of the two *k*'s with the large *n* occured *after* desorption.

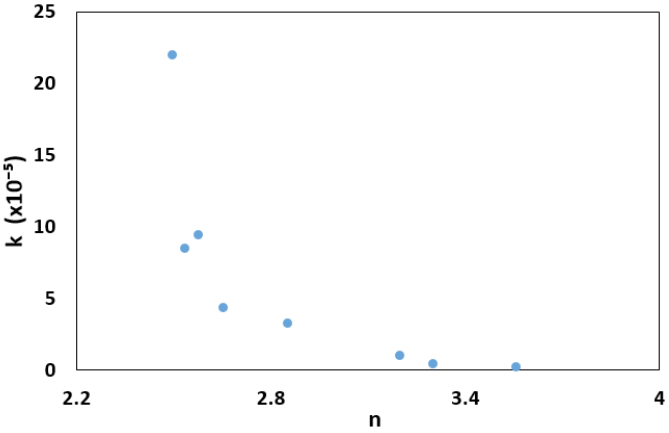

Figure 12. Plot of the Avrami *k* vs. *n* values for 1,6-dichlorohexane/naphthalene bilayers. The best fit line is an expoentially decaying function: $k = 1.85\pm0.05\bullet10^{-5}e^{-3.84\pm0.05n}s^{-1}$ and has a R^2 = 0.96. This functional form of *k* vs. *n* fit the data for all the systems. See the text regarding the slight variations.

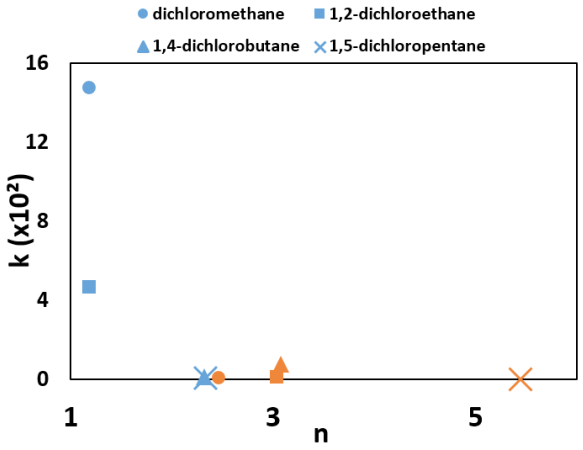

Figure 13. Plot of the Avrami *k* vs. *n* values for some of the bilayers. Shown in blue is the *k* and *n* for before desorption of the respective underlayer, and orange are the *k* and n for after desorption. Note that large *k* with small *n* is associated with shallow slope in the fluorescence intensity vs. T, whereas a small *k* with large *n* is associated with a steeper slope.